DOI: 10.1002/ejic.200601247

Mixed-Valent Linear Chain Pt_2PdPt_2 Complexes

Saiko Arai,[a] Masahiko Ochiai,[a] Koji Ishihara,*[a,b] and Kazuko Matsumoto*[a]

Keywords: Platinum / Palladium / Chain structures / Metal–metal interactions / Mixed-valent compounds

Pentanuclear linear-chain PtPd complexes $\{[Pt_2(NH_3)_2X_2(\mu\text{-pivalamidato})_2(CH_2COCH_3)]_2[PdX'_4]\}\cdot 2CH_3COCH_3$ (X = X′ = Cl (**1a**), X = Cl, X′ = Br (**1b**), X = Br, X′ = Cl (**1c**), X = X′ = Br (**1d**)) composed of a monomeric Pd^{II} complex sandwiched by two amidato-bridged dimeric Pt^{III} units were synthesized from the reaction between the acetonyl dinuclear Pt^{III} complexes having equatorial halide ligands $[Pt_2(NH_3)_2X_2(\mu\text{-pivalamidato})_2(CH_2COCH_3)]X''$ (X = Cl (**2a**), Br (**2b**), X″ = NO_3^-, $CH_3C_6H_4SO_3^-$) and $K_2[PdX'_4]$ (X′ = Cl, Br). The X-ray crystallographic analysis of **1a**–**1d** shows that the complexes have metal–metal bonded linear Pt_2PdPt_2 structures. The pentanuclear PtPd complexes have either an arch backbone structure or a sigmoid backbone structure, depending on the solvent of crystallization. The UV/Vis/NIR spectra clearly show the existence of a rare charge-transfer band from Pd to Pt in the pentanuclear PtPd complexes.

Introduction

Discrete metal chains composed of direct metal–metal interactions are of current interest from both theoretical and practical points of view.[1] One of the synthetic methods for this class of compounds is based on ligand-assisted metal–metal bond formation reactions by using polydentate ligands.[2,3] In this case, the number of the available coordination atoms of the ligand determines the length of the metal–metal chain. One of the representative cases is the family of metal string complexes supported by oligo-α-pyridylamido ligands.[2] A second approach involves the formation of metal–metal bonds by oxidation of d^8 square-planar complexes or by reduction of d^7 octahedral complexes, in which mixed-valent metal chain complexes are formed, such as platinum,[4–6] rhodium, and iridium blues.[7] The latter approach recently successfully extended the chain length to infinity, and allowed the isolation of the rare rhodium[8] and platinum one-dimensional mixed-valence compounds.[9,10] One-dimensional infinite platinum chain compounds,[11–13] such as Magnus' green salt[12] are another well known class of compounds, in which the metal–metal bond interactions rely upon self-stacking of square-planar complexes. Apart from these approaches, we previously reported pentanuclear Pt chain complexes $\{[Pt_2(NH_3)_2X_2(\mu\text{-pivalamidato})_2(CH_2COCH_3)]_2[PtX'_4]\}\cdot n CH_3COCH_3$ (X = X′ = Cl, n = 2 (**3a**), X = Cl, X′ = Br, n = 1 (**3b**), X = Br, X′ = Cl, n = 2 (**3c**), X = X′ = Br, n = 1 (**3d**))[14] having Pt–Pt···Pt···Pt–Pt structures with strong Pt^{III}···Pt^{II} interactions between the Pt^{III} dinuclear and $[PtX'_4]^{2-}$ units. The pentanuclear structures are maintained even in solution.

The number of Pd^{III} complexes that have been isolated and characterized is very limited, compared to the number of the mixed-valence Pt(II,III) chain species such as platinum blues.[4–6] Although paddlewheel compounds are known for most of the transition elements, there are only two types of structurally characterized Pd compounds having Pd^{III}_2 cores.[15] Palladium hardly makes a Pd^{III}–Pd^{III} σ bond based on the d_{z^2}–d_{z^2} overlap; if any it would be hard to observe experimentally.[15c] Attempts to generate a seemingly less difficult heterodinuclear $Pt^{III}Pd^{III}$ system have so far failed; oxidation of the dinuclear $Pt^{II}Pd^{II}$ complex $[(X_2)Pt(1\text{-MeU})_2Pd(Y_2)]Z$ (X_2, Y_2 = $(NH_3)_2$, en, or bpy; Z = $(NO_3)_2$, $(ClO_4)_2$, or SO_4) resulted in cleavage of the dinuclear complex into mononuclear Pt^{IV} and Pd^{II} complexes.[16] The dinuclear $Pt^{II}Pd^{II}$ complexes with Pt→Pd dative bonds, *trans*-$[(RNH_2)_2Pt(amidato)_2PdCl]^+$ (R = H, CH_3) or *trans*-$[(RNH_2)_2Pt(amidato)_2Pd(NH_3)]^{2+}$ (R = H, CH_3), have been reported, in which the coordination planes of Pt and Pd are perpendicular to each other and Pd is coordinated by Pt.[17] Only two trinuclear $Pt^{II}Pd^{III}Pt^{II}$ complexes with charge transfer from Pt to Pd have been reported, in which Pt–Pd σ bonds by the d_{z^2}–d_{z^2} overlap are involved.[18]

We report here the synthesis of the novel pentanuclear PtPd complexes $\{[Pt_2(NH_3)_2X_2(\mu\text{-pivalamidato})_2(CH_2COCH_3)]_2[PdX'_4]\}\cdot 2CH_3COCH_3$ (X = X′ = Cl (**1a**), X = Cl, X′ = Br (**1b**), X = Br, X′ = Cl (**1c**), X = X′ = Br (**1d**)) and $\{[Pt_2(NH_3)_2Cl_2(\mu\text{-pivalamidato})_2(CH_2COCH_3)]_2[PdCl_4]\}\cdot H_2O$ (**1a′**) having Pt–Pt–Pd–Pt–Pt structures with strong Pt–Pd interactions maintained by novel charge transfer from Pd to Pt (Scheme 1).

[a] Department of Chemistry, Advanced Research Center for Science and Engineering, Waseda University,
Okubo, Shinjuku-ku, Tokyo 169-8555, Japan
[b] Advanced Research Institute for Science and Engineering, Waseda University,
Okubo, Shinjuku-ku, Tokyo 169-8555, Japan
Supporting information for this article is available on the WWW under http://www.eurjic.org or from the author.

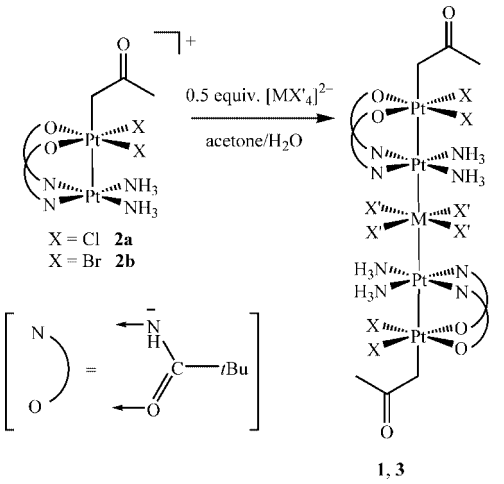

Scheme 1.

Results and Discussion

Synthesis and Characterization

The pivalamidato-bridged pentanuclear linear chain Pt_2PdPt_2 complexes **1a**–**1d** were synthesized in the same way as **3a**–**3d**[14a] from the reaction of 2 equiv. of **2a** or **2b** with 1 equiv. of $K_2[PdX'_4]$ (X′ = Cl, Br). The FAB-MS spectra of **1a**–**1d** showed the presence of molecular ions of **1a**–**1d**. Considering the fact that weak bonds such as ionic bonds are usually fragmented in FAB-MS spectra, the Pt···Pd interactions between the dinuclear units and the mononuclear unit seem to be substantially strong. The $^{195}Pt\{^1H\}$ NMR spectroscopic data of **1a**, **1d**, and related compounds including **3a** and **3d** are listed in Table 1. In Table 1, only one signal was observed for **1d**, and the satellite signals due to Pt–Pt coupling were not observed for **3a**, whereas all the signals were observed for **1a** and **3d**. The ^{195}Pt NMR spectra of **1a** and **3d** are shown in Figure 1. For **1a** and **3d**, the least-shielded signals at δ = 269 ppm (**1a**) and –230 ppm (**3d**) can be assigned to the $Pt(X_2O_2)$ atom (the elements in the parenthesis are coordination atoms), while the more- and most-shielded signals at δ = –2173 ppm (**1a**) and –2254 ppm (**3d**), and –2689 ppm (**3d**) can be assigned to the $Pt(N_4)$ and the $Pt(Br_4)$, according to the results of the ^{195}Pt NMR measurements for the related amidato-bridged Pt^{III} dinuclear complexes.[14,19] In fact, the peaks at δ = –2173 ppm (**1a**) and –2254 ppm (**3d**), and –2689 ppm (**3d**) are broader than those at δ = 269 ppm (**1a**) and –230 ppm (**3d**), and would be caused by quadrupole moments of the N atom and Br atoms [the nuclear spin quantum numbers (*I*) of ^{14}N and ^{81}Br are 1 and 3/2, respectively] coordinated to the Pt atom. The assignment of the broad peaks at δ = –2173 ppm (**1a**) and –2254 ppm (**3d**) is also supported by the fact that the $Pt(N_4)$ peak is split and most broadened because of the Pt–Pd (**1a**) or Pt–Pt (**3d**) coupling in addition to the Pt–N coupling. In **1d**, the peak of the $Pt(N_4)$ was more broadened than the corresponding $Pt(N_4)$ peak in **3d** because of the coupling with the Pd atom (^{105}Pd, I = 5/2).

Table 1. The ^{195}Pt NMR chemical shifts of the pentanuclear complexes and related compounds.

Complexes[a]	Coordinated atoms	$\delta(^{195}Pt)$ [ppm]
1a[b]	Cl_2O_2	269
	N_4	–2173
	Cl_4	ND
1d[b]	Br_2O_2	–231
	N_4	ND
	Br_4	ND
3a[b]	Cl_2O_2	268
	N_4	–2208
	Cl_4	–1888
3d[b]	Br_2O_2	–230
	N_4	–2254
	Br_4	–2689
2a[c]	Cl_2O_2	253
	N_4	–2080
2b[c]	Br_2O_2	–241
	N_4	–2122
$K_2[Pt^{II}Cl_4]$[d]	Cl_4	–1623
$K_2[Pt^{II}Br_4]$[d]	Br_4	–2672

[a] PVM: $(CH_3)_3CCONH$; X′′′ = p-$CH_3C_6H_4SO_3^-$, NO_3^-. [b] Measured in $[D_6]$acetone/D_2O (9:1), and locked with D_2O in an inner tube. [c] Measured in $[D_6]$acetone, and locked with D_2O in an inner tube. [d] Measured in D_2O.

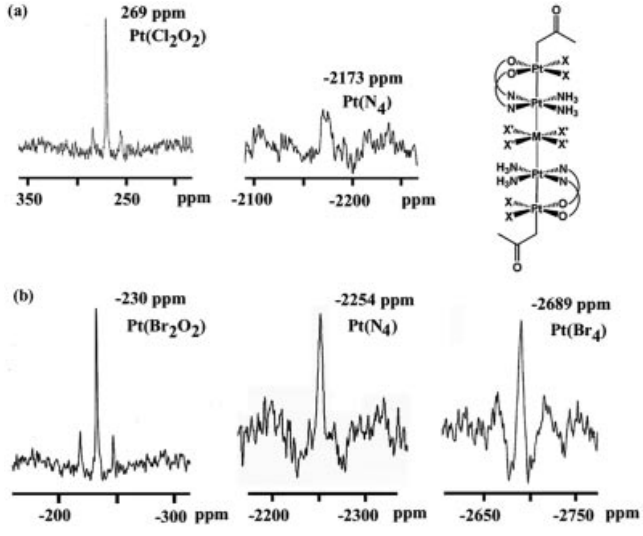

Figure 1. The ^{195}Pt NMR spectra of the pentanuclear PtPd complex (**1a**) and the pentanuclear Pt complex (**3d**): (a) $\{[Pt_2(NH_3)_2Cl_2(\mu\text{-pivalamidato})_2(CH_2COCH_3)]_2[PdCl_4]\}\cdot 2CH_3COCH_3$ (**1a**), (b) $\{[Pt_2(NH_3)_2Br_2(\mu\text{-pivalamidato})_2(CH_2COCH_3)]_2[PdBr_4]\}\cdot 2CH_3COCH_3$ (**3d**).

The broadenings caused by the couplings suggest that the Pt_2MPt_2 (M = Pt, Pd) backbones are retained even in solution. The UV/Vis/NIR spectra also showed the formation of the Pt_2PdPt_2 structures in the reaction solutions (see below).

Gradual evaporation of acetone from the reaction solution of **1a** gave two types of complexes from the same reaction solution, one with the arch structure (**1a**) and another

with the sigmoid structure (**1a′**). Crystallization of **1b** gave only one product as orange microcrystals because **1b** was quickly evaporated to avoid decomposition to black precipitate. The FAB-MS spectrum of the orange microcrystals showed the presence of molecular ions, and the elemental analysis approximately corresponded to **1b** with two molecules of acetone solvent. Crystallizations of **1c** and **1d** were carried out similarly to **1a**, however, **1c** and **1d** gave complexes of the arch structure and the sigmoid structure, respectively. In the case of **1d**, black precipitate was also obtained.

Crystal Structures

The X-ray structures of **1a** and **1a′** are shown in Figure 2. The structural parameters of **1a**, **1a′**, **1c**, **1d**, and **4b** are listed in Table 2. We have already reported that the equatorial halide ligands in the dimer units of **3a**–**3d** polarize the $R–Pt^{III}–Pt^{III}$ (R is acetonyl) in the amidato-bridged dimer approximately to $R–Pt^{IV}–Pt^{II}$ and induce the electron transfer from the monomer unit to the dimer units having the axial acetonyl ligands to stabilize the Pt–Pt bonds between the dimer and monomer units.[14,20] The same polarization of the Pt–Pt bonds in the dimer units of **1a**, **1a′**, **1c**, and **1d** is considered to work similarly in the pentanuclear structures of **1a**, **1a′**, **1c**, and **1d**. Such polarization of the Pt–Pt bonds in the dimer units is proved by the ^{195}Pt NMR spectra of both PtPd and PtPt complexes.

Two types of PtPd backbones, the arch structure (**1a**) and the sigmoid structure (**1a′**), were obtained from the same mother liquor as mentioned above. We previously reported that **3a** also had both arch and sigmoid backbones,[14a] but they were obtained from different mother liquors. In the present case, **1a**, which has two acetone molecules of crystallization, is formed preferentially from the mother liquor when acetone is moderately evaporated, while **1a′** is preferentially formed when the evaporation of acetone is either depressed or very rapid. In the crystals of **1a** two molecules of the arch PtPd complex exist facing each other probably by hydrophobic interaction. In the crystals of **1a** the pentanuclear Pt_4Pd molecules are regularly arranged by both intermolecular hydrophobic and hydrophilic interactions. As will be mentioned later, once-separated and redissolved solutions of **1a** and **1a′** showed the same spectral and chemical behavior. So the formation of **1a** and **1a′** would be explained as follows. The symmetrical sigmoid structure of **1a′** would be energetically favored and exist predominantly in the acetone-rich aqueous solution, because **1a′** would be favorably solvated by the moderately polar solvent, acetone in acetone-rich aqueous solution. So **1a′** crystallizes out by itself when the evaporation of acetone does not occur or occurs rapidly. On the other hand, in view of the fact that solubilities of **1a** and **1a′** into water are very low, **1a′** cannot gain such solvation energy in acetone-poor aqueous solution, so that **1a′** transforms into **1a** to gain stabilization energy from intermolecular interaction. Thus, when acetone evaporates gradually to make

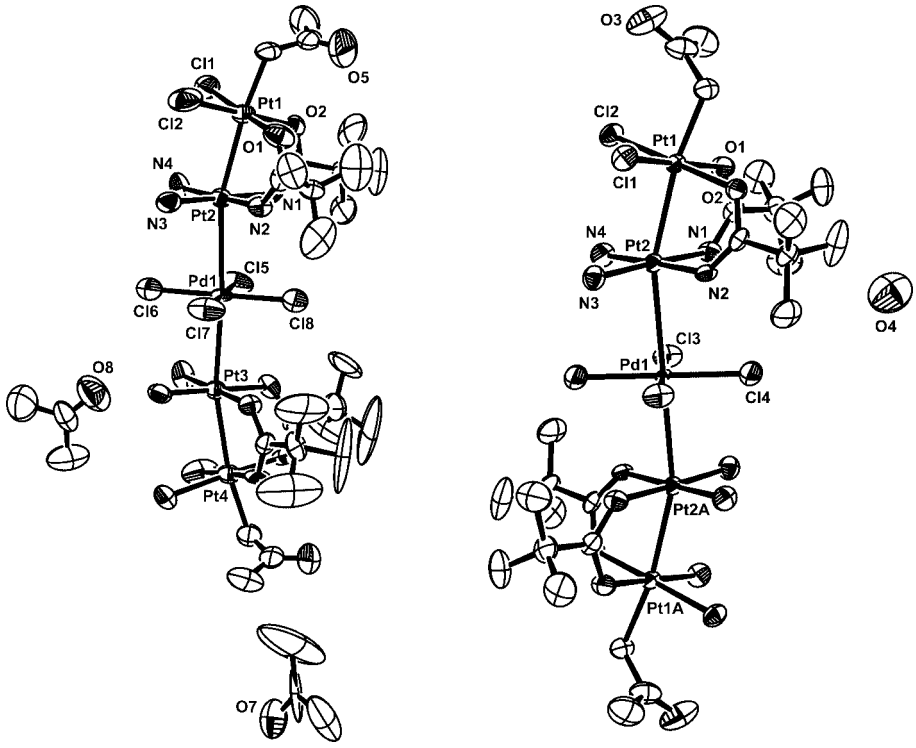

Figure 2. Crystal structures of the arch PtPd backbone complex (**1a**) and the sigmoid PtPd backbone complex (**1a′**): (a) $\{[Pt_2(NH_3)_2Cl_2(\mu\text{-pivalamidato})_2(CH_2COCH_3)]_2[PdCl_4]\}\cdot 2CH_3COCH_3$ (**1a**), (b) $\{[Pt_2(NH_3)_2Cl_2(\mu\text{-pivalamidato})_2(CH_2COCH_3)]_2[PdCl_4]\}\cdot H_2O$ (**1a′**). H atoms are omitted for clarity.

Table 2. Selected structural parameters of **1a**, **1a′**, **1c**, **1d**, and **4b**.[a]

	1a	**1a′**	**1c**	**1d**	**4b**
Bond lengths [Å]					
Pt1–Pt2	2.6895(19)	2.6924(11)	2.7188(19)	2.7100(9)	2.7182(10)
Pt2–$M_{monomer}$	3.030(2)	3.0319(14)	3.061(3)	3.1424(7)	3.3818(10)
Pt1–X1	2.280(7)	2.292(2)	2.413(3)	2.410(2)	2.4180(19)
Pt1–X2	2.270(8)	2.299(3)	2.423(3)	2.4113(17)	2.4034(19)
Pt1–C_{axial}	2.08(2)	2.092(9)	2.10(2)	2.089(12)	2.083(15)
$M_{monomer}$–L_{av}[b]	2.291(7)	2.312(3)	2.325(6)	2.4458(18)	2.072(14)
Bond angles [°]					
Pt1–Pt2–$M_{monomer}$	164.53(5)	162.724(17)	165.42(5)	162.79(2)	164.99(3)
Form[c]	A	S	A	S	A

[a] The parameters for Pt4 and Pt5 are close to those of Pt1 and Pt2, and therefore are omitted. [b] L = Cl (**1a**, **1a′**, and **1c**), Br (**1d**), NO_2 (**4b**). [c] The Pt backbone: arch (A), sigmoid (S).

the acetone-rich aqueous solution into an acetone-poor aqueous solution, **1a** comes out.

In the previous paper, it was concluded that the charges of the Pt atoms in **3a**–**3d** are not delocalized as in the platinum blues[4–6] but are localized approximately to $Pt^{III}_2Pt^{II}Pt^{III}_2$. The distances of $Pt(N_4)$–$Pt(X_4)$ [3.0054(11)–3.1109(15) Å] in **3a**–**3d** are significantly shorter than the $Pt(N_4)$–$Pt(Cl_4)$ distance (3.24 Å)[9] in Magnus' green salt, so the interactions between $Pt(N_4)$ and $Pt(X_4)$ are stronger in **3a**–**3d**, though the distances are slightly longer than a typical Pt–Pt single bond. However, it was found in the present study that the charges of the Pt atoms in **1a**, **1a′**, **1c**, **1d**, **4b**, and **3a**–**3d** are much more delocalized through the Pt backbones, as shown by the UV/Vis/NIR spectra (see below).

The X-ray structure of $[Pt_2(NH_3)_2Br_2(\mu\text{-pivalamidato})_2(CH_2COCH_3)]_2[Pt(NO_2)_4]$ (**4b**) is shown in Figure S3 (Supporting Information). The structural parameters of **4b** are listed in Table 2. The distances of $Pt(N_4)$–$Pt(X_4)$ in **4b** are too long to be a significant Pt–Pt interaction, so **4b** would not have a Pt–Pt bond between the monomer unit and the dimer units (see below).

Observation of Charge Transfers with UV/Vis/NIR Measurements

Long-wavelength absorption bands are known for the mixed-valence species such as tetranuclear platinum blues (λ_{max} = about 500 nm and 680–750 nm)[5] and the octanuclear platinum blue (λ_{max} = 540 nm and 1140 nm).[6] In these platinum blues, the latter bands are assigned to intervalence excitation from the inner Pt–Pt σ orbital to the inner Pt–Pt σ* orbital.[5c,6c] The present pentanuclear Pt_4Pd complexes **1a**–**1d** also have the intervalence charge transfer (IVCT) bands, which are similar to those of **3a**–**3d** (Table 3).

The absorption spectra of **2a** and $K_2[PdCl_4]$ are shown in Figure 3. The broad band (λ_{max} = 423 nm) in the $K_2[PdCl_4]$ spectrum is assigned to Cl → Pd LMCT transitions.[21] Complex **2a** has two strong absorption bands at λ_{max} = 325 and 434 nm. The former band is assigned to Pt → Pt MMCT transitions as judged from the comparison with other amidato-bridged Pt^{III} dinuclear complexes,[22] and the latter is assigned to Cl → Pt LMCT transitions. Obviously, there is no absorption band above 650 nm in the spectra. Figure 4 shows the time course of the UV/Vis/NIR spectral change during the reaction between **2a** and $K_2[PdCl_4]$ in aqueous acetone solution. The spectral change shows the process of **1a** formation. Little occurred until about 7 h after mixing, when the reaction started with a gradual rise of the IVCT absorption band at λ_{max} = 735 nm, and was complete after about 10 h. This absorption band was also observed when the crystals of **1a** or **1a′** were dissolved into the aqueous acetone solvent, and both solutions of **1a** and **1a′** showed an identical spectrum.

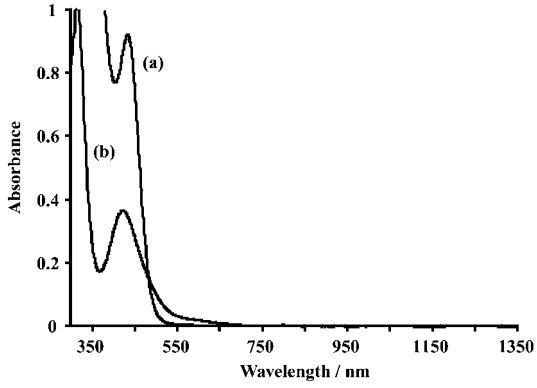

Figure 3. The UV/Vis/NIR spectra of **2a** and $K_2[PdCl_4]$: (a) acetone/water (9:1) solution of **2a** (4.5×10^{-4} M), (b) aqueous solution of $K_2[PdCl_4]$ (2.5×10^{-3} M).

Table 3. Absorption bands of **1a**–**1d** and **3a**–**3d** at various conditions.[a]

	1a, **1a′**	**1b**	**1c**	**1d**	**3a**	**3b**	**3c**	**3d**
Solution	735	763	724	808, 1014	770	810	792	835
Crystal (arch)	780			801	847		801	825
Crystal (sigmoid)	808					844		

[a] All values are displayed as λ_{max} (nm).

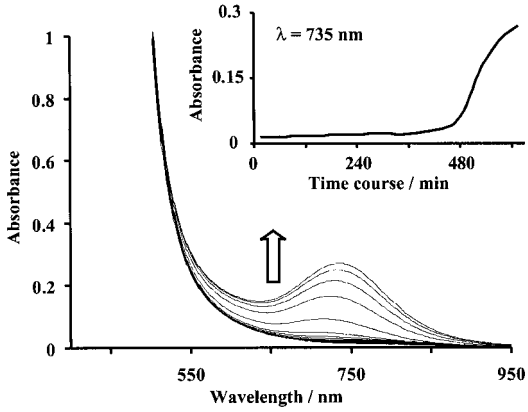

Figure 4. The time-course UV/Vis spectra for the pentanuclear PtPd backbone formation of **1a**. Spectra were recorded every 30 min after mixing solutions (a) and (b) in a quartz cell with 5-mm pathlength at room temperature. (a) 1.8 mL of the acetone solution of **2a** (1.0×10^{-2} M), (b) 0.2 mL of the aqueous solution of $K_2[PdCl_4]$ (4.5×10^{-2} M).

After reaction completion, the solution of **1a** was several-fold diluted and the spectrum was measured as shown in Figure 5. It is obvious that the original absorption bands at λ_{max} = 382 and 735 nm remain up to about 30-fold dilution. It is noteworthy that the Pt–Pd σ bonds are kept even in such a dilute solution of 1.5×10^{-4} M.

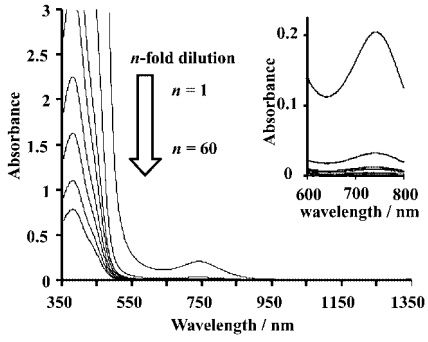

Figure 5. The UV/Vis/NIR spectra of **1a** with different concentrations. The acetone/water (9:1) solution of **1a** (4.5×10^{-3} M) was *n*-fold diluted with acetone/water (9:1) mixed solvent: n = 1 (no dilution), 5, 10, 15, 20, 30, 40, and 60.

Similar measurements were carried out for **1b**–**1d** and **3a**–**3d**, and similar results were obtained (see Figures S4–S17, Supporting Information).

The diffuse reflectance spectra of the microcrystals of **1a** and **1a′** in the range of 200–2000 nm were measured, and are shown in Figure 6 along with the spectra of **2a** and $K_2[PtCl_4]$. Figure 6 clearly shows the IVCT absorption band at around 850 nm. Complexes **3a**–**3d** and **1b**–**1d** also show the IVCT bands, as shown in Figures S18 and S19.

Recently, sensitivity of diffuse reflectance spectroscopy has greatly improved. We used the Kubelka–Munk transformation,[23] which can convert a reflectance spectrum into a spectrum similar to a conventional absorption spectrum for solution samples, to compare the reflectance and absorption spectra to each other. According to the Kubelka–Munk theory,[23] the Kubelka–Munk function $F(R_\infty)$ is

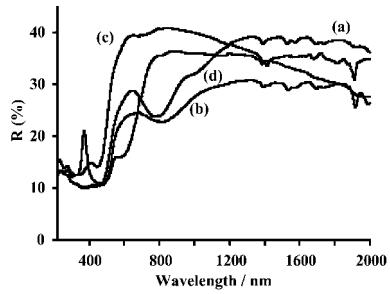

Figure 6. The diffuse reflectance spectra of **3a**, **2a**, K_2PtCl_4, and **1a**: (a) red-orange crystals of **3a**, (b) yellow powders of **2a**, (c) pale red powders of $K_2[PtCl_4]$, (d) yellow-orange crystals of **1a**.

given by the following equation for "infinitely thick" layers. In the equation R_∞ is the absolute reflectance for an infinitely thick sample and k is the absorption coefficient of the layer at a given wavelength,

$$F(R_\infty) = \frac{(1-R_\infty)^2}{2R_\infty} = \frac{k}{S} = \frac{\varepsilon c}{S}$$

S is the scattering coefficient (depending on the size and form of the particles), ε is the molar extinction coefficient of the analyte, and c is the molar concentration. The converted Kubelka–Munk spectra and the absorption spectra of **1a** and **1a′** in solution are shown in Figure 7 (see also Figures S20, S21 in the Supporting Information).

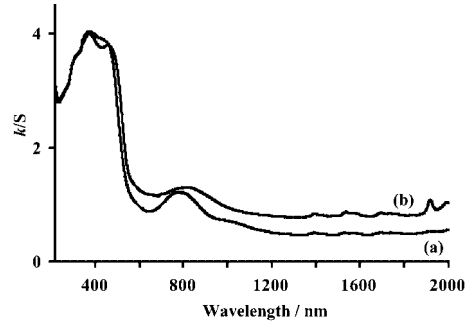

Figure 7. The transformed diffuse reflectance spectra of **1a** and **1a′**: (a) the arch PtPd backbone structure of **1a**, (b) the sigmoid PtPd backbone structure of **1a′**.

The band of the sigmoid backbone structure **1a′** in Figure 7 appeared at a longer wavelength than the arch one (**1a**), probably because the overlaps of d_{z^2} orbitals of Pt and Pd in **1a′** are more linear and therefore more efficient than in **1a**. The close similarity of the spectra in Figures 7 and 5 supports the assumption that the pentanuclear Pt_2MPt_2 structure is maintained, even in dilute solution.

Synthetic Elucidation of the Charge Transfer

In our previous article[14a] it was shown by the DFT calculation for **3a**–**3d** that the Pt···Pt interactions consist of the electron transfer from the monomer to the dimers. In the present study we prepared several pentanuclear Pt_4Pd complexes with different mononuclear complexes to examine

whether the same electron transfer as in **3a**–**3d** exists in **1a**–**1d** or not.

According to the DFT calculation of **3a**–**3d**, the p orbitals of halide ligands of the monomer unit, especially p_y orbital, donate electrons to the $Pt(X_4)$, and the d_{z^2} orbital of the $Pt(X_4)$ donates electrons to the Pt dimeric units.[14a] The π donor ability of the halide ligands would play a role in the electron flows through the Pt chains.

At first, we tried to prepare the pentanuclear analogues by using $[M(dmit)_2]^{2-}$ (M = Pt, Pd; dmit = 2-thioxo-1,3-dithiole-4,5-dithiolate) as a monomer complex, in which dmit is a σ donor and weak π acceptor contrary to halide ligands.[24] The metal complexes with dmit ligand are used to prepare charge transfer (CT) complexes similar to the organic CT compounds, such as BEDT-TTF, a well-known molecular metal and molecular superconductor.[25] As a result, pentanuclear complexes could not be synthesized, because dmit is a weak π acceptor.

In another attempt, we used $[M(CN)_4]^{2-}$ (M = Pt, Pd) as a monomer complex. CN^- is a weaker σ donor and weaker π acceptor than dmit.[24] The monomeric complex $K_2[Pt(CN)_4]$ is used to prepare the well-known Krogmann salt (KCP).[11] No pentanuclear complex was synthesized from the reaction of **2a** or **2b** with $[M(CN)_4]^{2-}$ (M = Pt, Pd), as shown in the VIS/NIR spectra (Figure S22).

Further, we used the NO_2^- ligand, which is a weaker σ donor and weaker π acceptor than the CN^- ligand.[24] Arch-like poor crystals of **4a** and needle crystals of **4b** were obtained. The former crystals would be $[Pt_2(NH_3)_2Cl_2(\mu\text{-pivalamidato})_2(CH_2COCH_3)]_2[Pt(NO_2)_4]$ (**4a**), though the structure could not be confirmed by X-ray analysis because of their poor crystallinity. The latter was $[Pt_2(NH_3)_2Br_2(\mu\text{-pivalamidato})_2(CH_2COCH_3)]_2[Pt(NO_2)_4]$ (**4b**), as confirmed by X-ray analysis. The distances of $Pt(N_4)$–$Pt(X_4)$ in **4b** are too long to be significant Pt–Pt interactions (about 3.4 Å), and correspondingly the reaction solutions did not show any absorption bands in the NIR region (Figures S23 and S24). The relative bulkiness of NO_2^- compared with halide would not be responsible for the long $Pt(N_4)$–$Pt(X_4)$ distance, because the coordination planes of the dimer units and the monomer unit are rotated to each other in a staggered form, as in all other pentanuclear complexes, to avoid steric hindrance among the coordinating ligands (Figure 8). The FAB-MS spectrum of the saturated solution of **4b** shows the small peaks of its molecular ion.

Thus, it seems that $[PtX'_4]^{2-}$, as well as other mononuclear complexes with ligands having considerable π donor ability, can form pentanuclear complexes, and the electron flow from the $Pd(X_4)$ to the $Pt(N_4)$ creates a strong Pt_{dimer}–$Pd_{monomer}$ interaction in **1a**–**1d**, which is similar to the interaction of Pt_{dimer}–$Pt_{monomer}$ in **3a**–**3d**.

Concluding Remarks

Novel linear pentanuclear complexes having Pt_2PdPt_2 chain backbones have been synthesized from the reaction between the amidato-bridged Pt^{III} dimer complexes and $[PdX_4]^{2-}$. The pentanuclear complexes are composed of two units of the amidato-bridged Pt^{III} dimer complexes sandwiching one unit of $[PdX_4]^{2-}$. The interactions between the Pt^{III} dimer units and the Pd^{II} monomer unit are strong enough to hold the linear pentanuclear chain structure retained in solution. The UV/Vis/NIR spectra clearly showed the charge transfer from the π donor chloride ligands of the Pd or Pt monomer unit to the Pt^{III} dinuclear units with axial acetonyl ligands. Such charge transfer from Pd to Pt is quite rare, and in fact multinuclear complexes involving a Pd→Pt dative bond are not known. It is noteworthy that the Pd–Pt bond is maintained even in highly diluted solution.

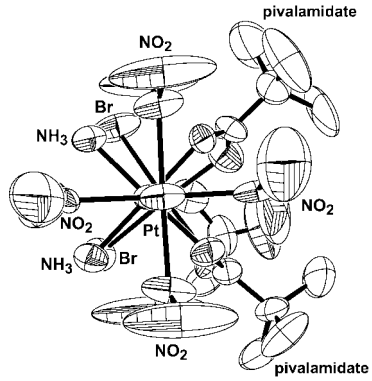

Figure 8. The structure of $[Pt_2(NH_3)_2Br_2(\mu\text{-pivalamidato})_2(CH_2COCH_3)]_2[Pt(NO_2)_4]$ (**4b**) viewed along the Pt axis from the monomer unit to the dimer unit.

Experimental Section

Materials and Methods: All the reactions and manipulations were performed in air and in the dark. Solvents were used as received. All the reagents were purchased from commercial sources and used as received. The complexes, $[Pt_2(NH_3)_2X_2\{(CH_3)_3CCONH\}_2(CH_2COCH_3)]X''$ (X = Cl, X'' = NO_3^- or $CH_3C_6H_4SO_3^-$ (**2a**), X = Br, X'' = NO_3^- or $CH_3C_6H_4SO_3^-$ (**2b**)), $[\{Pt_2(NH_3)_2X_2\{(CH_3)_3CCONH\}_2(CH_2COCH_3)]_2\}][PtX'_4]\cdot n CH_3COCH_3$ (X = X' = Cl, *n* = 2 (**3a**), X = Cl, X' = Br, *n* = 1 (**3b**), X = Br, X' = Cl, *n* = 2 (**3c**), X = X' = Br, *n* = 1 (**3d**)), and $K_2[Pt(NO_2)_4]$, were prepared as reported.[14,26]

Elemental analyses were carried out on a Perkin–Elmer PE 2400II. The ^1H NMR spectra were recorded with a JEOL Lambda 270 spectrometer and a Bruker AVANCE 400 spectrometer operating at 270 MHz and 400 MHz for ^1H, respectively. The $^{195}Pt\{^1H\}$ NMR spectra were recorded with a JEOL Lambda 500 spectrometer operating at 107.3 MHz for ^{195}Pt. Chemical shifts are in δ unit (parts per million, ppm) referenced to $(CD_3)_2CO$ at δ = 2.04 ppm for ^1H and to $H_2[PtCl_6]$ (external reference, 0 ppm) or $K_2[PtCl_4]$ (external reference, –1622 ppm) for ^{195}Pt. The mass spectra were measured with a JEOL JMS-SX102A spectrometer (FAB) and Thermo Quest LCQ-Deca spectrometer (ESI). The UV/Vis/NIR absorption spectra were measured with a JASCO Ubest V-570 with a cell holder for 5-mm pathlength. The diffuse reflectance spectra were measured with a JASCO Ubest V-570 with the custom-tailored integrating sphere unit.

Preparation of {[$Pt_2(NH_3)_2Cl_2$(μ-pivalamidato)$_2(CH_2COCH_3)$]$_2$-[$PdCl_4$]}·$2CH_3COCH_3$ (1a): A solution of **2a** (0.02 mmol) in acetone (2.0 mL) was added into an aqueous solution of $K_2[PdCl_4]$ (6.52 mg, 0.02 mmol, in 0.4 mL of water). The color of the reaction solution immediately changed from yellow to red. Yellow-orange crystals were obtained by slow evaporation of acetone in the dark. Yield: 8.49 mg, 45% (as crystals). $C_{32}H_{74}Cl_8N_8O_8PdPt_4$ (1869.3): C 20.56, H 3.99, N 5.99; found C 20.48, H 3.67, N 5.54. ^{1}H NMR (400 MHz, [D$_6$]acetone, 23 °C): δ = 5.20 (s, 4 H, CH_2), 2.25 (s, 6 H, CH_3), 1.16 (s, 36 H, CH_3). FAB-MS (positive) 1753.1 (molecule + H^+).

Preparation of {[$Pt_2(NH_3)_2Cl_2$(μ-pivalamidato)$_2(CH_2COCH_3)$]$_2$-[$PdCl_4$]}·H_2O (1a′): Dark orange crystals of **1a′** were obtained from the mother solution of **1a**. The evaporation conditions to sort the conformation of the PtPd backbones are shown in the text. Yield: 9.61 mg, 54% (as crystals). $C_{26}H_{64}Cl_8N_8O_7PdPt_4$ (1771.2): C 17.63, H 3.64, N 6.33; found C 17.65, H 3.43, N 6.05. ^{1}H NMR (400 MHz, [D$_6$]acetone, 23 °C): δ = 5.20 [s, ^2J(Pt,H) = 78.8 Hz, 4 H, CH_2], 2.26 (s, 6 H, CH_3), 1.17 (s, 36 H, CH_3) ppm.

Preparation of {[$Pt_2(NH_3)_2Cl_2$(μ-pivalamidato)$_2(CH_2COCH_3)$]$_2$-[$PdBr_4$]}·$2CH_3COCH_3$ (1b): The reaction solution of complex **1b** was prepared by the reaction of **2a** with $K_2[PdBr_4]$ (10.08 mg, 0.02 mmol). Orange microcrystals were obtained by speedy evaporation with a rotary evaporator to avoid decomposition. Yield 10.17 mg, 53%. $C_{32}H_{74}Br_4Cl_4N_8O_8PdPt_4$ (2047.1): C 18.77, H 3.64, N 5.47; found C 18.74, H 3.17, N 4.89. ^{1}H NMR (400 MHz, [D$_6$]-acetone, 23 °C): δ = 5.22 (s, 4 H, CH_2), 2.26 (s, 6 H, CH_3), 1.21 (s, 36 H, CH_3). FAB-MS (positive) 1931.9 (molecule + H^+).

Preparation of {[$Pt_2(NH_3)_2Br_2$(μ-pivalamidato)$_2(CH_2COCH_3)$]$_2$-[$PdCl_4$]}·$2CH_3COCH_3$ (1c): Complex **1c** was prepared in the same way as **1a** by the reaction of **2b** with $K_2[PdCl_4]$ (6.52 mg, 0.02 mmol), and was obtained as yellow-orange crystals. Yield 8.88 mg, 43% (as crystals). $C_{32}H_{74}Br_4Cl_4N_8O_8PdPt_4$ (2047.1): C 18.77, H 3.64, N 5.47; found C 18.82, H 3.69, N 5.19. ^{1}H NMR (400 MHz, [D$_6$]acetone, 23 °C): δ = 5.27 [s, ^2J(Pt,H) = 84.0 Hz, 4 H, CH_2], 2.28 (s, 6 H, CH_3), 1.17 (s, 36 H, CH_3). FAB-MS (positive) 1932.0 (molecule + H^+).

Preparation of {[$Pt_2(NH_3)_2Br_2$(μ-pivalamidato)$_2(CH_2COCH_3)$]$_2$-[$PdBr_4$]}·$2CH_3COCH_3$ (1d): Complex **1d** was prepared in the same way as **1a** by the reaction of **2b** with $K_2[PdBr_4]$ (10.08 mg, 0.02 mmol), and was obtained as red-orange crystals. Yield 5.27 mg, 24% (as crystals). $C_{32}H_{74}Br_8N_8O_8PdPt_4$ (2224.9): C 17.27, H 3.35, N 5.04; found C 17.02, H 3.28, N 4.85. ^{1}H NMR (400 MHz, [D$_6$]acetone, 23 °C): δ = 5.30 (s, 4 H, CH_2), 2.28 (s, 6 H, CH_3), 1.19 (s, 36 H, CH_3). FAB-MS (positive) 2109.3 (molecule + H^+).

Preparation of [$Pt_2(NH_3)_2Cl_2$(μ-pivalamidato)$_2(CH_2COCH_3)$]$_2$-[$Pt(NO_2)_4$] (4a): Complex **4a** was prepared in the same way as **1a** by the reaction of **2a** with $K_2[Pt(NO_2)_4]$ (2.29 mg, 0.005 mmol), and was obtained as poor yellow arch crystals. Yield 1.26 mg, 13% (as poor crystals).

Preparation of {[$Pt_2(NH_3)_2Br_2$(μ-pivalamidato)$_2(CH_2COCH_3)$]$_2$-[$Pt(NO_2)_4$]}·$2CH_3COCH_3$ (4b): Complex **4b** was prepared in the same way as **1a** by the reaction of **2b** with $K_2[Pt(NO_2)_4]$ (4.57 mg, 0.01 mmol). $C_{29}H_{68}Br_4N_{12}O_{15}Pt_5$ (2178.0): C 16.43, H 3.23, N 7.93; found C 16.79, H 3.13, N 7.19. FAB-MS (positive) 2062.8 (molecule + H^+).

X-ray Structure Determination: The data were collected on a Bruker SMART 1000 CCD diffractometer. The cell parameters were determined by using the programs SMART[27] and R-LATT.[28] Data reduction and integration were performed with the software package SAINT,[29] whereas the absorption collection was applied by using the program SADABS.[30] The structures were solved by full-matrix least-squares on F^2, and were refined with SHELXTL.[31] Hydrogen atoms were added in the idealized positions. Non-hydrogen atoms were refined with anisotropic temperature parameters. The crystal data are given in Table 4.

CCDC-631866 (for **1a**), -631865 (for **1a′**), -631867 (for **1c**), -631868 (for **1d**), and -631869 (for **4b**) contain the supplementary crystallographic data for this paper. These data can be obtained free of charge from The Cambridge Crystallographic Data Centre via www.ccdc.cam.ac.uk/data_request/cif.

Supporting Information (see also the footnote on the first page of this article): Full tables of the data collection parameters, anisotropic temperature factors, and bond lengths and angles for **1a**, **1a′**, **1c**, **1d**, and **4b**. Crystal structures of **1b**, **1c**, and **1d** are included. The UV/Vis/NIR spectra are also available.

Acknowledgments

We wish to express our thanks for financial support from the 21COE "Practical Nano-Chemistry" project from MEXT, Japan and from a Waseda University Grant for Special Research Projects.

Table 4. Crystallographic data for **1a**, **1a′**, **1c**, **1d**, and **4b**.

	1a	**1a′**	**1c**	**1d**	**4b**
Empirical formula	$C_{32}H_{74}Cl_8N_8O_8PdPt_4$	$C_{26}H_{62}Cl_8N_8O_8PdPt_4$	$C_{32}H_{74}Br_4Cl_4N_8O_8PdPt_4$	$C_{32}H_{74}Br_8N_8O_8PdPt_4$	$C_{32}H_{74}Br_8N_8O_8Pt_5$
M_r	1869.35	1785.20	2047.19	2225.03	2178.12
Crystal system	orthorhombic	monoclinic	orthorhombic	monoclinic	monoclinic
Space group	$Pca2_1$	$P2_1/n$	$Pca2_1$	$P2_1/c$	$P2_1/c$
a [Å]	24.291(17)	13.021(7)	24.663(18)	11.286(2)	16.052(4)
b [Å]	15.362(11)	12.158(6)	15.531(12)	23.260(5)	15.546(4)
c [Å]	15.478(11)	15.949(8)	15.568(11)	11.185(2)	25.731(7)
β [°]		97.731(9)		92.22(3)	106.072(4)
V [Å^3]	5776(7)	2502(2)	5963(8)	2934.1(10)	6170(3)
Z	4	2	4	2	4
$\rho_{calcd.}$ [g cm^{-3}]	2.150	2.370	2.280	2.519	2.345
T [K]	296(2)	296(2)	296(2)	296(2)	296(2)
μ Mo-K_α [mm^{-1}]	10.375	11.970	12.551	15.296	13.949
Gof	1.042	1.044	1.023	0.995	0.950
R_1, wR_2	0.0507, 0.0919	0.0292, 0.0729	0.0567, 0.1305	0.0540, 0.1143	0.0562, 0.1242

[1] a) J. K. Bera, K. R. Dunbar, *Angew. Chem. Int. Ed.* **2002**, *41*, 4453–4457 and references cited therein; b) P. Pyykkö, *Chem. Rev.* **1997**, *97*, 597–636; c) J. S. Miller (Ed.), *Extended Linear Chain Compounds*, Plenum Press, New York, **1982**, vols. 1–3.

[2] Selected references: a) J. F. Berry in *Multiple Bonds Between Metal Atoms*, 3rd ed. (Eds.: F. A. Cotton, C. A. Murillo, R. A. Walton), Springer Science and Business Media, Inc., New York, **2005**, pp. 669–706; b) I.-W. P. Chen, M.-D. Fu, W.-H. Tseng, J.-Y. Yu, S.-H. Wu, C.-J. Ku, C.-H. Chen, S.-M. Peng, *Angew. Chem. Int. Ed.* **2006**, *45*, 5814–5818.

[3] a) E. Goto, R. A. Begum, S. Zhan, T. Tanase, K. Tanigaki, K. Sakai, *Angew. Chem. Int. Ed.* **2004**, *43*, 5029–5032; b) T. Murahashi, M. Fujimoto, M. Oka, Y. Hashino, T. Uemura, Y. Tatsumi, Y. Nakao, A. Ikeda, S. Sakaki, H. Kurosawa, *Science* **2006**, *313*, 1104–1107; c) B. Osukui, W. S. Sheldrick, *Eur. J. Inorg. Chem.* **1999**, 1325–1333; d) B. Osukui, M. Mintert, W. S. Sheldrick, *Inorg. Chim. Acta* **1999**, *287*, 72–81; e) R. Usón, A. Laguna, M. Laguna, J. Jiménez, P. G. Jones, *Angew. Chem. Int. Ed. Engl.* **1991**, *30*, 198–199; f) A. Laguna, M. Laguna, J. Jiménez, F. J. Lahoz, E. Olmos, *Organometallics* **1994**, *13*, 253–257; g) T. Tanase, *Bull. Chem. Soc. Jpn.* **2002**, *75*, 1407–1422.

[4] a) S. J. Lippard, *Science* **1982**, *218*, 1075–1082; b) K. Matsumoto in *Cisplatin Chemistry and Biochemistry of a Leading Anticancer Drug* (Ed.: B. Lippert), Wiley-VCH, New York, **1999**, pp. 455–475; c) K. Matsumoto, K. Sakai, *Adv. Inorg. Chem.* **1999**, *49*, 375–427 and references cited therein.

[5] a) J. K. Barton, H. N. Rabinowitz, D. J. Szalda, S. J. Lippard, *J. Am. Chem. Soc.* **1977**, *99*, 2827–2829; b) J. K. Barton, C. Caravana, S. J. Lippard, *J. Am. Chem. Soc.* **1979**, *101*, 7269–7277; c) A. P. Ginsberg, T. V. O'Halloran, P. E. Fanwick, L. S. Hollis, S. J. Lippard, *J. Am. Chem. Soc.* **1984**, *106*, 5430–5439; d) T. V. O'Halloran, P. K. Mascharak, I. D. Williams, M. M. Roberts, S. J. Lippard, *Inorg. Chem.* **1987**, *26*, 1261–1270; e) K. Sakai, Y. Tanaka, Y. Tsuchiya, K. Hirata, T. Tsubomura, S. Iijima, A. Bhattacharjee, *J. Am. Chem. Soc.* **1998**, *120*, 8366–8379.

[6] a) K. Sakai, K. Matsumoto, *J. Am. Chem. Soc.* **1989**, *111*, 3074–3075; b) K. Sakai, K. Matsumoto, K. Nishio, *Chem. Lett.* **1991**, 1081–1084; c) K. Matsumoto, K. Sakai, K. Nishio, Y. Tokisue, R. Ito, T. Nishide, Y. Shichi, *J. Am. Chem. Soc.* **1992**, *114*, 8110–8118.

[7] a) C. Tejel, M. A. Ciriano, B. E. Villarroya, J. A. López, F. J. Lahoz, L. A. Oro, *Angew. Chem. Int. Ed.* **2003**, *42*, 529–532; b) C. Tejel, M. A. Ciriano, L. A. Oro, *Chem. Eur. J.* **1999**, *5*, 1131–1135 and references cited therein; c) B. E. Villarroya, C. Tejel, M.-M. Rohmer, L. A. Oro, M. A. Ciriano, M. Bénard, *Inorg. Chem.* **2005**, *44*, 6536–6544.

[8] a) G. M. Finniss, E. Canadell, C. Campana, K. R. Dunbar, *Angew. Chem. Int. Ed. Engl.* **1996**, *35*, 2772–2774; b) M. E. Prater, L. E. Pence, R. Clérac, G. M. Finniss, C. Campana, P. Auban-Senzier, D. Jérome, E. Canadell, K. R. Dunbar, *J. Am. Chem. Soc.* **1999**, *121*, 8005–8016; c) M. P. Doyle, T. Ren, *Prog. Inorg. Chem.* **2001**, *49*, 113–168; d) F. A. Cotton, E. V. Dikarev, M. A. Perukhina, *J. Organomet. Chem.* **2000**, *596*, 130–135; e) F. A. Cotton, E. V. Dikarev, M. A. Perukhina, *J. Chem. Soc., Dalton Trans.* **2000**, 4241–4243; f) F. P. Pruchnik, P. Jakimowicz, Z. Ciunik, K. Stanislawek, L. A. Oro, C. Tejel, M. A. Ciriano, *Inorg. Chem. Commun.* **2001**, *4*, 19–22.

[9] a) K. Sakai, E. Ishigami, Y. Konnno, T. Kajiwara, T. Ito, *J. Am. Chem. Soc.* **2002**, *124*, 12088–12089; b) K. Sakai, M. Takeshita, Y. Tanaka, T. Ue, M. Yanagisawa, M. Kosaka, T. Tsubomura, M. Ato, T. Nakano, *J. Am. Chem. Soc.* **1998**, *120*, 11353–11363.

[10] a) K. Uemura, K. Fukui, H. Nishikawa, S. Arai, K. Matsumoto, *Angew. Chem. Int. Ed.* **2005**, *44*, 5459–5464; b) K. Uemura, K. Fukui, K. Yamasaki, K. Matsumoto, *Sci. Technol. Adv. Mater.* **2006**, *7*, 461–467; c) W. Chen, F. Liu, D. Xu, K. Matsumoto, S. Kishi, M. Kato, *Inorg. Chem.* **2006**, *45*, 5552–5560.

[11] a) K. Krogmann, *Angew. Chem. Int. Ed. Engl.* **1969**, *8*, 35–42; b) J. S. Williams, A. J. Schultz, A. E. Underhill, K. Carneiro in *Extended Linear Chain Compounds* (Ed.: J. S. Miller), Plenum Press, New York, **1982**, vol. 1, pp. 73–118; c) S. Yamada, *Bull. Chem. Soc. Jpn.* **1951**, *24*, 125–127.

[12] a) M. Atoji, J. W. Richardson, R. E. Rundle, *J. Am. Chem. Soc.* **1957**, *79*, 3017–3020; b) J. R. Miller, *J. Chem. Soc.* **1965**, 713–720; c) H. J. Keller, in *Extended Linear Chain Compounds* (Ed.: J. S. Miller), Plenum Press, New York, **1982**, vol. 1, pp. 357–407; d) J. Bremi, W. R. Caseri, P. Smith, *J. Mater. Chem.* **2001**, *11*, 2593–2596; e) W. Caseri, *Platinum Met. Rev.* **2004**, *48*, 91–100 and references cited therein.

[13] a) M. Yamashita, S. Takaishi, A. Kobayashi, H. Kitagawa, H. Matsuzaki, H. Okamoto, *Coord. Chem. Rev.* **2006**, *250*, 2335–2346 and references cited therein; b) K. Otsubo, A. Kobayashi, H. Kitagawa, M. Hedo, Y. Uwatoko, H. Sagayama, Y. Wakabayashi, H. Sawa, *J. Am. Chem. Soc.* **2006**, *128*, 8140–8141; c) H. Kitagawa, T. Mitani, *Coord. Chem. Rev.* **1999**, *190–192*, 1169–1184; d) J. Ohara, S. Yamamoto, *Phys. Rev. B* **2006**, *73*, 045122-1-7.

[14] a) K. Matsumoto, S. Arai, M. Ochiai, W. Chen, A. Nakata, H. Nakai, S. Kinoshita, *Inorg. Chem.* **2005**, *44*, 8552–8560; b) F. Liu, W. Chen, D. Wang, *Dalton Trans.* **2006**, 3445–3453.

[15] a) F. A. Cotton, I. O. Koshevoy, P. Lahuerta, C. A. Murillo, M. Sanaú, M. A. Ubeda, Q. Zhao, *J. Am. Chem. Soc.* **2006**, *128*, 13674–13675; b) F. A. Cotton, J. Gu, C. A. Murillo, D. Timmons, *J. Am. Chem. Soc.* **1998**, *120*, 13280–13281; c) J. F. Berry, E. Bill, E. Bothe, F. A. Cotton, N. S. Dalal, S. A. Ibragimov, N. Kaur, C. Y. Liu, C. A. Murillo, S. Nellutla, J. M. North, D. Villagrán, *J. Am. Chem. Soc.* **2007**, *129*, 1393–1401; d) J. F. Berry, F. A. Cotton, S. A. Ibragimov, C. A. Murillo, X. Wang, *Inorg. Chem.* **2005**, *44*, 6129–6137.

[16] a) W. Micklitz, J. Riede, B. Huber, G. Müller, B. Lippert, *Inorg. Chem.* **1988**, *27*, 1979–1986; b) K. Matsumoto, H. Urata, *Chem. Lett.* **1993**, 2061–2064.

[17] a) C. Mealli, F. Pichierri, L. Randaccio, E. Zangrando, M. Krumm, D. Holtenrich, B. Lippert, *Inorg. Chem.* **1995**, *34*, 3418–3424; b) M. Krumm, B. Lippert, B. L. Randaccio, E. Zangrando, *J. Am. Chem. Soc.* **1991**, *113*, 5129–5130; c) M. Krumm, E. Zangrando, L. Randaccio, S. Menzer, B. Lippert, *Inorg. Chem.* **1993**, *32*, 700–712.

[18] a) W. Micklitz, G. Müller, J. Riede, B. Lippert, *J. Chem. Soc., Chem. Commun.* **1987**, 76–78; b) W. Micklitz, G. Müller, B. Huber, J. Riede, F. Rashwan, J. Heinze, B. Lippert, *J. Am. Chem. Soc.* **1988**, *110*, 7084–7092; c) A. Hegmans, E. Zangrando, E. Freisinger, F. Pichierri, L. Randaccio, C. Mealli, M. Gerdan, A. X. Trautweon, B. Lippert, *Chem. Eur. J.* **1999**, *5*, 3010–3018.

[19] a) S. Iwatsuki, E. Isomura, A. Wada, K. Ishihara, K. Matsumoto, *Eur. J. Inorg. Chem.* **2006**, 2484–2490; b) R. Z. Pellicani, F. P. Intini, L. Meresca, E. Mesto, C. Pacifico, G. Natile, *Eur. J. Inorg. Chem.* **2006**, 1635–1642; c) M. Sterzel, J. Autshbach, *Inorg. Chem.* **2006**, *45*, 3316–3324; d) W. Brüning, I. Ascaso, E. Freisinger, M. Sabat, B. Lippert, *Inorg. Chim. Acta* **2002**, *339*, 400–410; e) T. G. Appleton, K. A. Byriel, J. M. Garrett, J. R. Hall, C. H. L. Kennard, M. T. Mathieson, R. Stranger, *Inorg. Chem.* **1995**, *34*, 5646–5655.

[20] a) K. Matsumoto, M. Ochiai, *Coord. Chem. Rev.* **2002**, *231*, 229–238; b) M. Ochiai, K. Fukui, S. Iwatsuki, K. Ishihara, K. Matsumoto, *Organometallics* **2005**, *24*, 5528–5536; c) N. Saeki, N. Nakamura, T. Ishibashi, M. Arime, H. Sekiya, K. Ishihara, K. Matsumoto, *J. Am. Chem. Soc.* **2003**, *125*, 3605–3616; d) M. Ochiai, Y.-S. Lin, J. Yamada, H. Misawa, S. Arai, K. Matsumoto, *J. Am. Chem. Soc.* **2004**, *126*, 2536–2545; e) M. Arime, K. Ishihara, K. Matsumoto, *Inorg. Chem.* **2004**, *43*, 309–316; f) M. Ochiai, K. Matsumoto, *Chem. Lett.* **2002**, 270–271; g) Y.-S. Lin, H. Misawa, J. Yamada, K. Matsumoto, *J. Am. Chem. Soc.* **2001**, *123*, 569–575; h) Y.-S. Lin, S. Takeda, K. Matsumoto, *Organometallics* **1999**, *18*, 4897–4899; i) K. Matsumoto, Y. Nagai, J. Matsunami, K. Mizuno, T. Abe, R. Somazawa, J.

Kinoshita, H. Shimura, *J. Am. Chem. Soc.* **1998**, *120*, 2900–2907; j) K. Matsumoto, J. Matsunami, K. Mizuno, H. Uemura, *J. Am. Chem. Soc.* **1996**, *118*, 8959–8960.

[21] a) D. S. Martin Jr, in *Extended Linear Chain Compounds* (Ed.: J. S. Miller), Plenum Press, New York, **1982**, vol. 1, pp. 409–451; b) F. A. Cotton, G. Wilkinson, C. A. Murillo, M. Bochmann, *Advanced Inorganic Chemistry*, 6th ed., John Wiley & Sons, New York, **1999**.

[22] a) S. Iwatsuki, K. Ishihara, K. Matsumoto, *Sci. Technol. Adv. Mater.* **2006**, *7*, 411–424; b) S. Iwatsuki, C. Mizushima, N. Morimoto, S. Muranaka, K. Ishihara, K. Matsumoto, *Inorg. Chem.* **2005**, *44*, 8097–8104; c) K. Shimazaki, H. Sekiya, H. Inoue, N. Saeki, K. Ishihara, K. Matsumoto, *Eur. J. Inorg. Chem.* **2003**, 1785–1793; d) N. Saeki, Y. Hirano, Y. Sasamoto, I. Sato, T. Toshida, S. Ito, N. Nakamura, K. Ishihara, K. Matsumoto, *Eur. J. Inorg. Chem.* **2001**, 2081–2088; e) N. Saeki, Y. Hirano, Y. Sasamoto, I. Sato, T. Toshida, S. Ito, N. Nakamura, K. Ishihara, K. Matsumoto, *Bull. Chem. Soc. Jpn.* **2001**, *74*, 861–868.

[23] a) M. P. Fuller, P. R. Griffiths, *Anal. Chem.* **1978**, *50*, 1906–1910; b) S. A. Yeboah, S. Wang, P. R. Griffiths, *Appl. Spectrosc.* **1984**, *38*, 259–264; c) E. Péré, H. Cardy, O. Cairon, M. Simon, S. Lacombe, *Vib. Spectrosc.* **2001**, *25*, 163–175.

[24] a) R. H. Crabtree, *The Organometallic Chemistry of the Transition Metals*, 4th ed., Wiley-Interscience, **2005**; b) F. A. Cotton, C. A. Murillo, R. A. Walton, *Multiple Bonds between Metal Atoms*, 3rd ed., Springer Science and Business Media, Inc., New York, **2005**; c) G. Aullón, S. Alvarez, *Inorg. Chem.* **1996**, *35*, 3137–3144; d) T. Yamaguchi, F. Yamazaki, T. Ito, *J. Am. Chem. Soc.* **1999**, *121*, 7405–7406; e) T. Yamaguchi, F. Yamazaki, T. Ito, *J. Am. Chem. Soc.* **2001**, *123*, 743–744.

[25] P. Cassoux, L. Valde, H. Kobayashi, A. Kobayashi, R. A. Clark, A. E. Underhill, *Coord. Chem. Rev.* **1991**, *110*, 115–160.

[26] M. Vézes, *Bull. Soc. Chim. Fr.* **1899**, *21*, 481–487.

[27] *SMART for WindowsNT/2000*, *Version 5.625*, Bruker Advanced X-ray Solutions, Inc., Madison, WI, **2001**.

[28] *R-LATT*, *Reciprocal Lattice Viewer*, *Version 3.0*, Bruker Advanced X-ray Solutions, Inc., Madison, WI, **2000**.

[29] *SAINT*, *Data Reduction Software*, *Version 6.22*, Bruker Advanced X-ray Solutions, Inc., Madison, WI, **2001**.

[30] *SADABS*, *Area Detector Absorption and other Corrections Software*, *Version 2.03*, Bruker Advanced X-ray Solutions, Inc., Madison, WI, **2000**.

[31] G. M. Sheldrick, *SHELXTL*, *Version 5.1*, Bruker Advanced X-ray Solutions, Inc., Madison, WI, **1998**.

Received: December 26, 2006
Published Online: April 10, 2007

